Journal of Power Sources 251 (2014) 92–107

Contents lists available at ScienceDirect

Journal of Power Sources

journal homepage: www.elsevier.com/locate/jpowsour

Coal-fuelled systems for peaking power with 100% CO_2 capture through integration of solid oxide fuel cells with compressed air energy storage

Jake Nease, Thomas A. Adams II *

Department of Chemical Engineering, McMaster University, 1280 Main Street West, Hamilton, Ontario, Canada L8S 4L7

HIGHLIGHTS

- A CO_2 emission-free peaking power plant fuelled by gasified coal is discussed.
- The performances of 16 different plant configurations are quantified.
- The direct impact of a water–gas shift process step is investigated and analyzed.
- Peaking power from coal is possible using CAES with little only minor impacts on electricity costs.
- SOFC/CAES plants can be economically advantageous at high fuel or carbon prices.

ARTICLE INFO

Article history:
Received 20 June 2013
Received in revised form
15 November 2013
Accepted 16 November 2013
Available online 28 November 2013

Keywords:
Solid oxide fuel cells
Compressed air energy storage
Carbon capture
Peaking power
Coal

ABSTRACT

In this study, a coal-fuelled integrated solid oxide fuel cell (SOFC) and compressed air energy storage (CAES) system in a load-following power production scenario is discussed. Sixteen SOFC-based plants with optional carbon capture and sequestration (CCS) and syngas shifting steps are simulated and compared to a state-of-the-art supercritical pulverised coal (SCPC) plant. Simulations are performed using a combination of MATLAB and Aspen Plus v7.3. It was found that adding CAES to a SOFC-based plant can provide load-following capabilities with relatively small effects on efficiencies (1–2% HHV depending on the system configuration) and levelized costs of electricity ($\sim$0.35 ¢ kW^{-1} h^{-1}). The load-following capabilities, as measured by least-squares metrics, show that this system may utilize coal and achieve excellent load-tracking that is not adversely affected by the inclusion of CCS. Adding CCS to the SOFC/CAES system reduces measurable direct CO_2 emission to zero. A seasonal partial plant shutdown schedule is found to reduce fuel consumption by 9.5% while allowing for cleaning and maintenance windows for the SOFC stacks without significantly affecting the performance of the system ($\sim$1% HHV reduction in efficiency). The SOFC-based systems with CCS are found to become economically attractive relative to SCPC above carbon taxes of \$22 ton^{-1}.

1. Introduction

On the global scale, the electricity generation industry is largely dependent on the use of fossil fuels such as natural gas and coal due to their high abundance and relative ease of access. Energy conversion with renewable fuel sources (wind, solar, bio-fuels etc.) is still decades away from being implemented on any significant scale. To illustrate, it is projected that the total electricity produced in the United States and Canada by renewable (non-hydro) sources in the year 2035 will be 16% and 10%, respectively [1,2]. Consequently, for the near term it is necessary to improve the performance of fossil-fuelled systems (both environmentally and economically) to drive society toward a sustainable future. Moreover, government incentives and emission restriction programs, such as cap-and-trade systems or taxes on equivalent CO_2 emissions may become a challenge for electricity providers in the coming years. To avoid these added costs, the electricity generation sector will be motivated to capture the CO_2 generated by their operations for underground sequestration (geological formation such as aquifers or depleted oil wells present viable options) or possibly resale as a value-added product for enhanced-oil recovery among other uses [3]. The coal-based power generation industry will thus be forced to develop and invest in CO_2 capture technology or pay the financial penalties that will accrue due to their emission to the atmosphere.

* Corresponding author. Tel.: +1 (905) 525 9140x24782.
E-mail address: tadams@mcmaster.ca (T.A. Adams).

0378-7753/$ – see front matter © 2013 Elsevier B.V. All rights reserved.
http://dx.doi.org/10.1016/j.jpowsour.2013.11.040

Either way, the impact to the end consumer will be increased electricity prices and therefore an increased cost of living.

In the interest of developing new methods to use coal for electricity generation, this work analyzes the performance of an integrated solid-oxide fuel cell (SOFC) and compressed air energy storage (CAES) plant, fuelled by gasified coal, that is capable of meeting demand variations (referred to hereafter as "peaking power"). The SOFC system uses gasified coal as the fuel source, and each of the designs are compared to a modern coal-based power process, the supercritical pulverized coal combustion process (SCPC). Sixteen system configurations with design decisions such as optional carbon capture and sequestration (CCS) and optional water–gas shift (WGS) reactors are considered.

1.1. Pulverized coal and gasification

Coal powers approximately 45% of the electricity generation in the United States and is expected to remain the dominant fuel choice through 2035 [1]. On a global scale, coal accounts for approximately 33% of all electricity production and is expected to maintain a significant share over the next few decades [4]. Coal-fired power plants produce an inherently high amount of CO_2 per unit of electricity generated (approximately 90.29 g MJ^{-1}) and therefore account for a significant amount of the CO_2 emissions in the power generation sector [5]. In 2010, coal-based processes contributed 80.9% of the total CO_2 emissions for the electricity generation sector in the United States, or 26.8% of all of the CO_2 emitted across all industries [6]. Reducing or eliminating the CO_2 emissions from coal-fed plants would contribute significantly towards the large-scale reduction of the United States' CO_2 emissions.

The SCPC process is chosen as the "status quo" coal-fed power generation process for the purposes of this investigation. The SCPC process is briefly described as follows [7]: coal is combusted with air in a boiler, generating heat to power steam turbines. Steam is generated above the critical point (hence "supercritical") at 240 bar and 593 °C to improve downstream power generation efficiency. The combustion products are mainly CO_2, H_2O, N_2, SO_2 and ash, as well as small amounts of other impurities (Hg, S, Cl). The ash and sulphur are removed through separate cleanup steps and the small amounts of impurities can be removed through various well-proven processes, yielding a final exhaust stream containing mainly H_2O, CO_2 and N_2. At this point, the exhaust can be vented to the atmosphere (as is typically done), or post-combustion CO_2 absorption may be performed to remove CO_2 for capture and sequestration purposes. Absorption can be performed with chemical solvents such as Monoethanolamine (MEA) or Methyldiethanol amine (MDEA), or physical solvent processes such as Rectisol™ or Selexol™. Approximately 90% of the CO_2 in the exhaust gas can be recovered at purities required for pipeline transport, with the rest being emitted to the atmosphere via the exhaust gas. Although they are effective, absorption-based CCS strategies are energy-intensive and often lead to prohibitive decreases in overall system efficiency, leading to higher electricity costs [7]. Other more recent approaches such as membrane-based processes, pressure swing adsorption and vacuum swing adsorption have also been investigated with promising results [8,9].

Gasified coal processes such as the integrated gasification combined cycle (IGCC) involve the gasification of coal into synthesis gas (syngas, CO and H_2) as well as CO_2 and H_2O. The water–gas shift (WGS) reaction can then be performed downstream of the gasification step to increase the amount of H_2 in the syngas stream. After gas shifting, the same solvent-based absorption processes for CCS can be employed to remove CO_2 before the downstream use of the syngas. As in the post-combustion CCS case, approximately 90% of the CO_2 in the syngas stream can be recovered at pipeline purity [7].

1.2. Solid oxide fuel cells

SOFCs make use of a hydrogen-based or carbonaceous fuel gas and an oxidant (air is typically used due to its availability and high oxygen content) to produce electricity through electrochemical reactions on either side of an impermeable partition, as depicted in Fig. 1. The reactions that occur in the anode and cathode are the oxidation of the fuel gas and the reduction of O_2, respectively. A sample of these reactions may include, but are not limited to, the following [10]:

$$H_2 + O^{=} \rightarrow H_2O + 2e^{-} \quad \text{(Anode)} \tag{1}$$

$$CO + O^{=} \rightarrow CO_2 + 2e^{-} \quad \text{(Anode)} \tag{2}$$

$$O_2 + 4e^{-} \rightarrow 2O^{=} \quad \text{(Cathode)} \tag{3}$$

SOFCs are fuel-flexible, and are able to utilize a variety of carbonaceous fuel sources. Examples of possible fuels include H_2 and CO (syngas), natural gas [11], methanol [12], jet fuel [12] and others [13]. Several other carbonaceous sources may be gasified, converted to syngas, and then used as a fuel source for the SOFC anode as well. Such options include coal [14], biomass [15,16], diesel [12] and others. See our prior work for a discussion of different fuel sources [13]. As shown in Fig. 1, the products on the anode side consist of H_2O, CO_2 and unspent fuel. If the anode and cathode outlet streams can be kept unmixed (which is possible), the anode products allow for simple and effective CCS to be employed. The unspent fuel in the anode exhaust may be combusted with stoichiometric amounts of O_2 (an excess of which may result in violating CO_2 pipeline restrictions) resulting in a mixture of nearly 100% CO_2 and H_2O. The CO_2 may then be captured at pipeline purities with minimal parasitic energy costs through a series of flash drums; see the patent by Adams and Barton (2009) for details [17]. The cathode exhaust contains mostly deoxygenized air at a high temperature (~900 °C) and pressure (10–20 bar), which facilitates several opportunities for additional power generation via a thermal (heat recovery steam generation (HRSG) cycle, for example) and/or pressure-driven (Brayton turbines, for example) bottoming cycle before being vented to atmosphere with essentially no environmental impact [10]. It has been shown in our prior work that gasified coal-fed SOFC processes can achieve electrical efficiencies of more than 45% by higher heating value (HHV) while completely capturing all CO_2 emissions [18,19]. Similar results have been obtained by other research groups (see Refs. [20–23] and Table 4 in Ref. [13], for example). The process of converting electrochemical potential to electricity is an inherently more efficient process than combustion, thus allowing for SOFC-based systems to make better

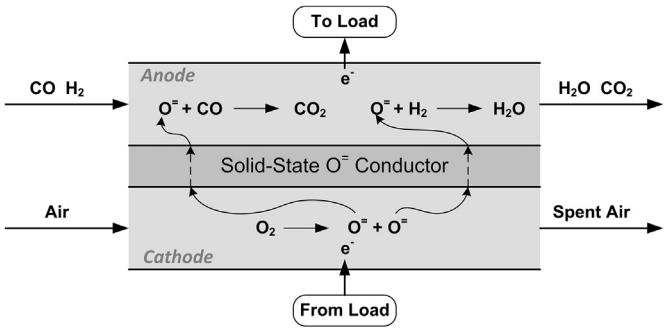

Fig. 1. Simple schematic of a SOFC using syngas as a fuel source with possible reactions shown. Reproduced from Ref. [10].

use of the energy contained within the resource than most modern commercially available technologies.

Although a very promising technology for bulk power generation, the SOFC is not without its disadvantages. A significant current limitation to SOFC technology is that there are cost-prohibitive challenges associated with operating the unit dynamically. For example, it is possible to attempt to provide peaking power by adjusting the power output from an SOFC stack in real time [24], but not without seriously risking cell degradation or destruction due to thermal expansion, gas backflow, and a variety of other problems [25]. Recent studies have shown that this remains an ongoing issue [26,27]. Therefore, we anticipate that future SOFC systems at the bulk scale will be used as fixed-output power suppliers that provide base-load power at high efficiency, with no capabilities of providing peaking power. It is possible to design an SOFC system to provide the maximum anticipated peak (and thereby always meet demand), but such a system would nearly always produce more electricity and consume more fuel than necessary.

1.3. Compressed air energy storage

CAES plants operate as intermittent sinks or sources of electrical power through the storage of mechanical energy in the form of compressed air. A CAES plant functions by consuming available electrical power to compress and store air as elastic potential energy in an above- or below-ground void. Typical storage voids may include depleted natural gas reserves, solution-mined salt domes and aquifers. The compressed air can then be pre-heated (typically by combusting it with natural gas) and released through expansion turbines attached to electrical generators in order to convert the stored elastic potential back into electrical power. CAES plants can be used as temporary storage options for large-scale processes that preclude the use of batteries or other distributed energy storage options, making it a prime candidate for bulk peaking power generation. A typical CAES system is shown diagrammatically in Fig. 2.

CAES is a mature technology that has successfully been utilized both in the United States and overseas for over 35 years. Examples of currently operating CAES plants include a 290 MW plant operated by E.N. Kraftwerke and a 110 MW plant operated by the Alabama Electric Company [28], alluding to the longevity and applicability of the technology. The two existing plants exploit the concept of peak electricity pricing; during periods of low electricity prices (night time), the CAES system consumes electricity, and re-feeds it to the electrical grid when the price of electricity is high (day time). The resulting arbitrage situation allows the CAES system to operate profitably. As of 2009, no other standalone CAES plants were planned on being constructed due to various issues [29]. However, in the summer of 2013 Apex announced an Award given to Dresser-Rand for a 317 MW system to be built in Texas valued at approximately $200 million, and another 270 MW facility from Chamisa Energy is scheduled to go online in 2014 [30,31].

Not only can a CAES system be used individually, but its rapid dynamics and controllability make it well-suited for combination with other process for added flexibility. One intriguing application of CAES is for the levelling of intermittent and somewhat unpredictable power generated by wind turbines in an attempt to provide reliable base-load power [28,32–37]. In much the same fashion, we feel that CAES can be used in an opposite role where it supplements an already reliable base load to provide controllable and reliable peaking power. There are two notable disadvantages to a CAES system: it requires an external electrical power source, and (in the absence of a significant heat sink), it requires the combustion of natural gas before (or in) the expansion turbines, resulting in CO_2 emissions.

1.4. Integration of SOFC and CAES systems

As an extension of our prior work, this study investigates the integration of gasified coal-fuelled SOFCs (to provide base-load power), a CCS system (to eliminate direct CO_2 emissions), and a CAES plant (to be used in an attempt to consume or supplement the base-load outlet, thereby resulting in peaking power), and is the first to do so to the best of our knowledge. As a further extension of our prior work, we quantify the impact of including the WGS step upstream of the SOFC stack on plant reliability and performance. The combined system exploits synergies that exist between each of the sections mentioned, effectively overcoming their individual disadvantages. The SOFC and CCS systems are modelled to be consistent with those of Adams and Barton (see Refs. [17–19,38]). The steady-state CAES model was kept the same as our prior work on natural gas systems with CAES for comparative purposes, but is applied with the process conditions of a SOFC plant fuelled by gasified coal. This SOFC/CAES/CCS system is capable of generating load-following power from gasified coal with essentially 100% carbon capture and high efficiencies relative to the current state-of-the-art. A simplified block diagram of the proposed integrated SOFC/CAES process is given in Fig. 3. A more detailed PFD of the proposed integrated process is provided in Fig. 4 and a more detailed model description is provided in Section 2.

In this work, we perform techno-economic, load following and overall system performance analyses of sixteen configurations of the integrated SOFC/CAES process described above. Aspen Plus v7.3 was used for the steady-state computations of mass and energy flows throughout the process, and in-house models implemented

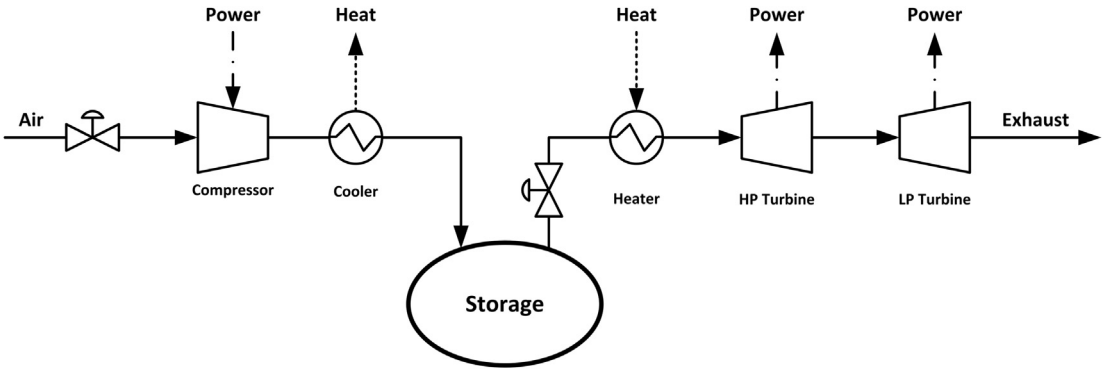

Fig. 2. Simplified CAES system schematic. Reproduced from Ref. [10].

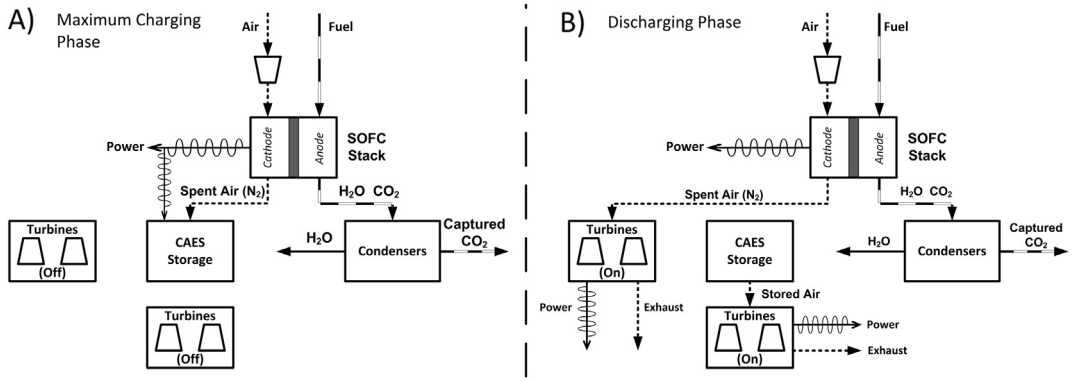

Fig. 3. Simplified SOFC/CAES integration technique during (A) the maximum charging phase, and (B) the discharging phase. Reproduced from Ref. [51].

in MATLAB were used for dynamic simulations performed using a pseudo steady-state approach. For load-following and economic performance evaluations, the historical power demand and price profiles for the province of Ontario, Canada in 2011 are used [39]. The boundaries for this analysis are the plant gates, and do not include transmission of electricity in or out of the plant, or the costs associated with the transport of fuels. These boundaries are chosen to be consistent with those of the NETL SCPC studies [7] to which the results are compared.

In this work, the SOFC/CAES system is shown to be a promising process which is able to produce load-following electric power from coal with very low direct and indirect CO_2 emissions. The CAES is shown to provide load-following abilities sufficient to the needs of actual grid behaviour at only a small price premium over baseline-only power generation using SOFCs. In addition, sensitivity analysis results show that the SOFC/CAES system can even be the best option from a pure economic point of view under certain realistic market conditions and carbon tax policies.

2. Simulation models

There have been several studies on the systems-level implementation of SOFCs and gas turbines for electricity generation using coal [20–23] or natural gas [40–45] as fuel sources (see Adams et al. (2012) for a review of these studies [13]). Detailed modelling decisions and assumptions for the SOFC model used in this work are available in Adams and Barton (2010); since this is an extension of our prior work, many of the same modelling parameters are used so that a meaningful comparison between the results may be drawn [18]. The SOFC model was integrated with a CAES process model to create the SOFC/CAES process presented in Fig. 4. Air separation, gasification and syngas cleaning, syngas shifting and impurity removal, power generation, heat recovery, and CO_2 recovery are the major components of the SOFC model. A brief description of each section is provided, but the reader is referred to our prior work for a more in-depth discussion [18]. The CAES system consists of compression, storage, and expansion models. The following sections give an overview of each of these process steps in turn.

2.1. Steady-state simulation and modelling approach

The SOFC was sized to target a base-load net power output of 719 MW when carbon capture is enabled (including the net power produced by the SOFCs, the bottoming expansion turbines utilizing stream 6.5 on the cathode side, and the HRSG). The US Department of Energy anticipates that MW-scale SOFC stacks will be available for demonstration by 2020, and therefore this scale of plant is considered to be reasonable for the forward-looking plant designs discussed in this work [46]. Multiple plant configurations are discussed in section 3. Each plant was scaled to achieve this same 719 MW output as the basis of comparison. The feedstock for this process was assumed to be Illinois #6 bituminous coal, which has a HHV of 27.267 MJ kg^{-1} [47]. By weight, the coal contains 63.75% C, 4.5% H, 1.25% N, 0.29% Cl, 2.51% S, 11.12% H_2O and the balance ash. Steady-state simulations of the SOFC/CAES system were performed in Aspen Plus v7.3 using the Peng–Robinson equation of state (EOS) with the Boston–Mathias modification with a few exceptions [48]: the NBC/NRC steam tables were used for pure water streams, the Electrolyte-NRTL method with Henry coefficients from the AP065 databank was used for streams consisting of mostly CO_2 and H_2O near the critical point of CO_2, and the Redlich–Kwong–Soave EOS with predictive Holderbraum mixing rules was used for streams containing mostly CO_2 and H_2O below the critical point of CO_2. A detailed discussion regarding the selection of each thermodynamic method and any other process assumptions (unless explicitly stated otherwise) for the portions of the process which do not involve CAES are available in our prior work [18].

2.2. Solid oxide fuel cell process model

2.2.1. Air separation

The air separation unit (ASU) serves to obtain high-purity oxygen from atmospheric air for use in various downstream process units. The majority of the separated O_2 is used in the gasifier, with small amounts also being used in the post-SOFC oxidation unit (stream 6.2 in Fig. 4) and the Claus unit for sulphur removal (stream 1.3 in Fig. 4). 94% of the oxygen in the feed air stream is recovered at 10 bar and 32.2 °C. The parasitic energy load of the ASU is accounted for by detracting from the steady-state base load of the plant. A more detailed description of this process and each unit is given in the prior work and is thus omitted here for the sake of brevity [18]. However, it is important to note that the ASU for this process was originally designed for an IGCC process in which the N_2 (which is a waste stream in this process) is used elsewhere in the process [7]. Consequently, it may be possible to improve the ASU process' efficiency by avoiding the production of high-pressure N_2, which is left as a future study in this work.

2.2.2. Gasification and syngas cleaning

The gasifier converts coal and water into syngas, which is modelled as a mixture of H_2, CO, H_2O, CO_2 and other gaseous impurities including N_2, Ar, HCl, COS, NH_2, Hg, CH_4 and H_2S. When possible, water is recycled to the gasifier from downstream processes, which contains small amounts of CO_2. The gasifier operates exothermically and the waste heat can be used for different

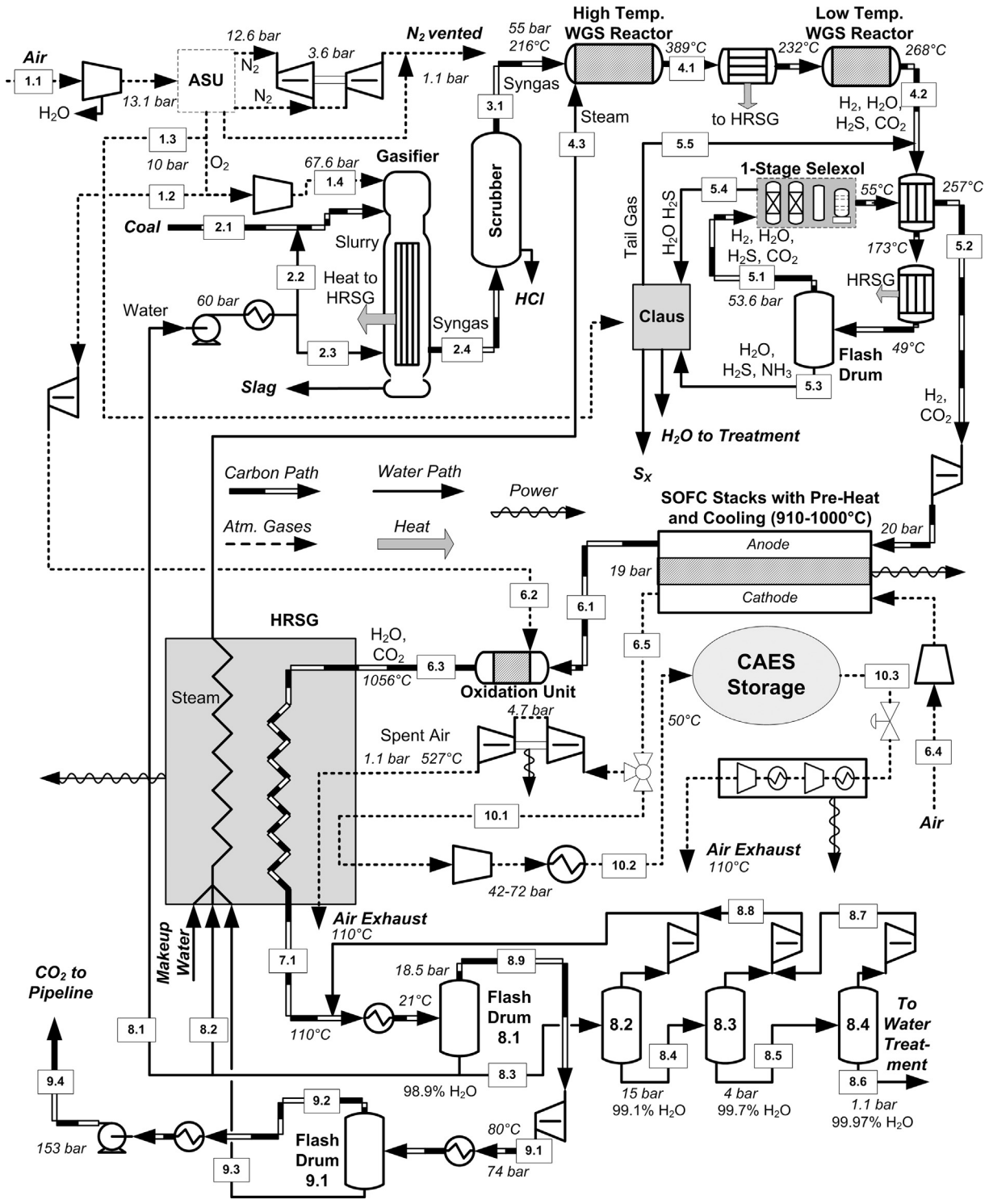

Fig. 4. PFD of proposed SOFC/CAES plant including optional WGS reactors, CAES storage/turbomachinery, and CCS.

purposes. For designs in which CAES is not used (i.e., the prior work [18]), the waste heat is used to generate steam for additional power generation in the HRSG. When CAES is enabled, some of the waste heat can instead be recovered for the pre-heating of the CAES discharge stream, which will be discussed in Section 2.3. Non-combustibles in the coal are recovered as a molten slag stream. To be consistent with our prior work and commonly used baseline studies [7], a GE Radiant-Only gasifier at 56 bar and 1300 °C was used. The syngas and slag product streams are assumed to be cooled to 210 °C before moving to any downstream processes. Further modelling details, including gasifier reactions, are given in our prior work [18].

SOFC stacks are very susceptible to impurities such as HCl and H_2S [49–51]. For simplicity, a detailed scrubbing step is omitted from this investigation, and 100% of the HCl produced in the gasifier is assumed to be removed. H_2S removal is described next.

2.2.3. Syngas shifting and impurity removal

After the syngas has been cleaned, it may optionally be sent to a water–gas shift (WGS) step in order to increase the H_2:CO ratio prior to entering the fuel cell. It is a subject of current debate as to whether or not the WGS step is required for SOFC systems, and it is not yet clear if future large-scale implementations of SOFCs will include this step during fuel preparation. Competing issues such as carbon deposition on the anode via the Boudouard equation, decreased theoretical cell voltage, sensitivity to sulfide poisoning depending on fuel gas CO content, exergetic losses, and increased capital costs must all be addressed before a consensus can be reached [52]. Therefore, in this study each system configuration was simulated both with and without the WGS step, which was not considered in our prior work.

When the WGS step is included most of the CO in the fuel stream is converted to CO_2 through two packed-bed reactors in series. First, a high-temperature (300–450 °C) reactor achieves about 80% conversion of the inlet CO, then a low-temperature (200–300 °C) reactor is assumed to reach chemical equilibrium, corresponding to an overall conversion of approximately 96%. One convenient side reaction that takes place in the WGS reactors is that of COS hydrolysis:

$$COS + H_2O \rightleftharpoons CO_2 + H_2S. \quad (4)$$

Due to the high H_2O:COS ratio in the WGS reactors, it is assumed that the COS hydrolysis reaction reaches 100% conversion. This is beneficial to the sulphur recovery step because H_2S is more easily recovered from the fuel stream than COS. Further design details (such as types of catalyst packing) and sample steady-state stream conditions are available in our prior work [18].

After the optional WGS step, impurities such as sulphur, ammonia and mercury must be removed prior to entering the SOFC anode. Mercury transport was not modelled in this investigation, and it is thus assumed that the trace amounts of mercury in the fuel stream are removed via a mercury removal process (not shown in Fig. 4). A one-stage Selexol process is used to remove H_2S (and any COS if a WGS step is not used) from the fuel stream because the SOFCs cannot tolerate sulphur concentrations higher than 100 ppm [53,54]. Since the fuel stream must be cooled to near-ambient conditions (49 °C) prior to entering the Selexol process, most of the NH_3 is condensed out with the entrained water vapour through a series of coolers and is sent to a Claus process for treatment. The Selexol process is designed to be able to remove 99.6% of the H_2S in the fuel stream [18]. The product sulphur stream is combusted with high-purity O_2 in a Claus furnace to form sulphur (S_x) compounds, with 4.2% of the H_2S present in the Claus process feed stream remaining unrecovered in the tail gas.

2.2.4. Power generation and heat recovery

The SOFC is the heart of this process and generates the bulk of the system's power through the electrochemical reactions (1), (2) and (3). It is assumed that the SOFC stacks operate at a 950 °C and 20 bar (primarily constrained by material limitations) [55]. The syngas leaving the impurity removal step (stream 5.2 in Fig. 4) is expanded to 20 bar, heated to 910 °C and fed to the anode of the fuel cell stack. Air obtained from the atmosphere is fed to the cathode at the same conditions after a compression and heating step. Separate anode and cathode exhausts prevent the mixing of N_2 and CO_2, promoting convenient CO_2 capture and sequestration (see Section 2.2.5) [10]. The anode exhaust is completely oxidized with high-purity O_2 provided by the ASU to mostly H_2O and CO_2 in a fuel completion step. The SOFC stack models were updated from Ref. [18] to account for the new design condition in two ways. First, the overall fuel utilization of the SOFC stacks was changed to 86% (from 99.5%). Second, the ideal cell voltage when the WGS step is omitted was lowered to 0.6 V to reflect the impact of H_2S (at approximately 20 ppm after the impurity removal step) on the anode in the presence of CO [51]. When running on near-pure H_2 (as is the case when the WGS step is included), the ideal cell voltage is maintained at 0.719 V [55]. It is assumed that 5% of the heat generated in the cell is lost to the surroundings, and that the DC/AC conversion is 96% efficient [53,55]. The proposed design uses six parallel SOFC trains such that each one can be turned off for a few months every three years for maintenance and seasonal power adjustments [10].

Table 1
Operating characteristics the CAES section of the proposed SOFC/CAES integrated system [53].

Operating condition	Value	Units
Air turbines (CAES power train in Fig. 4)		
Rated turbine power	200	MW
Maximum air flow rate	440	kg s^{-1}
Inlet pressure to HP turbine	40	bar
Inlet temperature to HP turbine	550	°C
Inlet pressure to LP turbine	6	bar
Inlet temperature to LP turbine	825	°C
Turbine efficiency	75	%
Compressor (compresses steam 10.1 in Fig. 4)		
Maximum air flow rate	210	kg°s^{-1}
Rated compressor power	140	MW
Temperature at exit of after-cooler	50	°C
Pressure at exit of after-cooler	42–73	bar
Compressor isentropic efficiency	75	%
Cavern		
Volume of storage space	600,000	m^3
Cavern operating pressures	40–72	bar
Maximum cavern pressure	72	bar
Cavern wall temperature	50	°C

After exiting the anode, the fuel exhaust stream (which still contains small amounts of CO and H_2) is sent to an adiabatic oxidation reactor where it is reacted with stoichiometric amounts of O_2, resulting in a stream consisting of almost entirely H_2O and CO_2. Before being sent to the CO_2 removal step, the heat contained in the anode exhaust is used to generate steam in the HRSG. The path of the cathode exhaust stream is dependent on the operational objective of the combined SOFC/CAES plant at any point in time. When the demand for electricity is below that of the plant's base load or its price is relatively low, the cathode exhaust is compressed beyond the 20 bar operating pressure of the SOFC to the necessary pressure for storage in the CAES cavern. When the price or demand for electricity is high, the cathode exhaust is sent to a steady-state bottoming cycle to recover as much energy as possible. In both cases, any excess thermal energy contained within the cathode stream is recovered via the HRSG.

The heat exchanger network (HEN) designs as well as the HRSG are modelled using a simple approach [18] and are not discussed here for the sake of brevity. However, the two main assumptions for this section are: (1) the HEN avoids temperature crossover but assumes an ideal minimum approach temperature of 0 °C, and (2) all waste heat between 110 and 950 °C is considered to be a useful heat source in the steam generation process. The techno-economic analysis presented in the results section includes all capital expenditures relating to the HRSG equipment.

2.2.5. CO_2 recovery and sequestration

Since the completed fuel stream is primarily CO_2 and H_2O, effective CO_2 separation can be obtained through a series of liquid/vapour flash unit operations after it is cooled in the HRSG [17].

Some of the high purity water that is recovered is used as make-up water for either process steam or power generation (via the HRSG). Surplus water is not considered in this analysis, but it may be treaded and used for other purposes if not released as a waste product. The CO_2 rich vapour is compressed to 74 bar and flashed once more to remove any remaining water, resulting in the CO_2 purity required for pipeline transit [56]. The CO_2 stream is compressed to a supercritical fluid and pumped to 153 bar before it leaves the plant for sequestration. Essentially 100% of the CO_2 in the incoming fuel stream is captured, and water is recovered at 99.97% purity.

2.3. Compressed air energy storage process and model

The CAES section was partially modelled in Aspen Plus in the same fashion as our prior work, with stream and unit connection adjustments made as necessary due to the differences between gasified coal- and natural gas-fed systems [10]. Moreover, the general design and operating parameters of the CAES process are typical of those used in other CAES literature, including those used in our prior investigation. These parameters are provided in Table 1, and further details describing the operation of the CAES system and its equipment selection can be found in our prior work but are omitted here for the sake of brevity [10,57,58].

2.4. Dynamic simulation modelling approach

The CAES dynamic modelling approach is modified from the approach developed in our prior work for natural gas fuelled SOFC/CAES systems [10] to adjust for the presence of coal fuels. A pseudo-steady-state model was used to account for the dynamics of the SOFC/CAES system. Streams and units that are considered transient involve those downstream of stream 6.5. In contrast, all units upstream of stream 6.5 and downstream of 6.1 (gasification and syngas shifting/cleanup, SOFC stacks, the CCS section, and related heat integration) are operated as a base-load plant and hence are not considered in the pseudo-steady-state model.

The goal of the pseudo-steady-state model is to compute the operating conditions of the SOFC/CAES at any given control interval. To do this, one-hour control intervals are used in which the system is assumed to achieve steady-state instantly and hold it for the hour. This is appropriate because accurate predictions of future power demand (up to 24 h in advance) are available at one hour increments [39] and because the compressor and turbine dynamics are very fast, requiring seconds to minutes to achieve major swings in power, [29,59].

At each control interval, the model must calculate the required flow rate of air to or from the cavern based on the power desired and the amount of air stored in the cavern. To do this with the rigorous Aspen Plus model requires an approximately 15 min of CPU time per control interval (Intel® Core-2 Quad @2.66 GHz and 7 GB RAM), or about 91 days per simulation. Instead, a reduced model was constructed by running the Aspen Plus model to generate a data table mapping the flow rate of air into the CAES cavern, the corresponding compressor pressure, and net operating power, and then fitting a nonlinear equation to that data. This brought the simulation time from 91 days to about 80 s. See the prior work for details such as the model structure and logical implementation [10].

2.5. Combined plant scenario and operational objectives

For the purposes of this study, it is assumed that the operational objective of the combined SOFC/CAES plant is to provide reliable peaking power for a large community (demand patterns ranging between 500 and 900 MW) that exhibits the same relative peaking load profile as the province of Ontario, Canada [39]. Consequently, historical market data for the province of Ontario for the calendar year of 2011 was scaled to a plant average of 719 MW and is used as the forecasted demand profile for dynamic simulations. Uncertainties and stochastic demand considerations are not considered; their impact on the optimal performance of the SOFC/CAES plant is left to future work. In the cases where the integrated SOFC/CAES system is incapable of providing the load demanded (whether due to operational constraints or the storage cavern being empty or unavailable), it is assumed that all supplementary power is purchased from the grid at the historical Ontario market price for that particular hour and day. Furthermore, it is assumed that a natural gas combined cycle (NGCC) peaking plant is used to generate any supplementary power and that it emits 50.29 g of CO_2-equivalents per MJ of electricity generated, which must be accounted for as an indirect emission of the proposed SOFC/CAES plant [61]. Finally, it is assumed that any power generated by the plant beyond the demanded load (for example, when the storage cavern is full and base-load operation is the only available mode of operation) is curtailed with no financial benefits (or penalties) to the plant.

This study associates the economic and load-following performance of the integrated SOFC/CAES plant using the following metrics [61]:

$$\mathrm{LCOE} = \sum_{t=0}^{N} \left(\frac{\frac{I_t + M_t + F_t}{(1+r)^t}}{\sum_{t=0}^{N} \frac{P_t}{(1+r)^t}} \right) \tag{5}$$

$$\mathrm{SSE} = \sum_{i=1}^{n} \left(P_{\mathrm{P},i} - D_i \right)^2 \tag{6}$$

$$\mathrm{WSSE} = \sum_{i=1}^{n} U_i^2 + \left(\frac{O_i}{2} \right)^2, \tag{7}$$

where LCOE, SSE and WSSE are the levelized cost of electricity, the sum of squared-errors, and the weighted sum of squared-errors between supply and demand. In the LCOE calculation I_t, M_t, F_t and P_t are the capital investment, maintenance costs, fuel costs and total sellable power produced in year t, respectively. The plant lifetime is N years (assumed to be 20 years) and is discounted at a real interest rate of r (10%). The variable D_i represents the demand at interval i over n time steps (1 h per time step for one year). O_i is the amount of power over-produced by the plant and U_i is the amount under-produced by the plant at time step i.

As is the case in industry, a balance is sought between economic, environmental and overall system performance. For these reasons, the LCOE is used to give insight into the economic performance of the proposed system configurations relative to each other and the current SCPC option. CO_2 emissions are accounted for using a carbon tax (which is the subject of a sensitivity analysis) and are reflected in the LCOE. The SSE and WSSE are used to compare the load-following capabilities of each system; the WSSE differs from the SSE in that it more heavily weights times when demand exceeds supply, and hence additional grid power must be purchased.

2.6. Case studies

Eighteen different plant configurations have been considered and their performances compared in each of the load-following scenario described in Section 2.5. The first two cases are standard SCPC plants scaled to a fixed output of 719 MW, one of which

includes CCS [7]. The SCPC plant using CCS is capable of 90% removal of CO_2 using a solvent-based technique [7]. The sixteen new cases that have been investigated involve every possible configuration of the SOFC/CAES plant incorporating any of the WGS step, CCS, and a train shut-down (TSD) schedule. A summary of the features of each case is given in Table 2. Simulation and financial calculation parameters are consistent with our prior work and are provided in Table 3 [10]. A base-case carbon tax of \$50/tonne of CO_2 emitted is considered, but is treated as a sensitivity variable in later analysis. Various carbon taxes of up to over \$100 tonnes^{-1} have been reported in other recent works [63,64]. Train shut-down involves the lowering of the plant's base-load output, and allows for consistent cleaning and maintenance of the SOFC stacks to be performed during periods of seasonally low demand while not affecting upstream units and saving fuel costs. The CAES system is able to, for the most part, meet the daily peaks during the seasons in which TSD is used, and any shortcomings are accounted for in the economic and performance analyses. See our prior work for more details [10].

Capital and operating cost results were obtained from making manual adjustments and using appropriate scaling factors in combination with Aspen Icarus cost estimation software, published cost estimates, and correlations provided by Seider et al. [65]. Unit sizing and justification can be found in our prior work and is not repeated here [18]. The most recent available target for FuelCell Energy's (a world leader in SOFC stack manufacturing) SOFC stack costs at maturity is \$317 kW^{-1} (US\$2007) and includes all accessories and balance-of-plant units for a 10 year stack lifetime [66]. Redox Power Systems, an emerging SOFC manufacturer, is targeting a release of their SOFC technology for purchase in 2014 at a cost of \$1000 kW^{-1} [67]. A price of \$500 kW^{-1} (requiring two stacks for a total of \$1000 kW^{-1} over the 20 year plant lifetime) is therefore assumed to be a conservative SOFC stack cost estimate for this future application. The CAES costs are those of the source wells, storage cavern construction, compressors, turbines and related heat equipment. The CAES plant is equal in size to our prior investigation, and hence the unit and process costs are the same as those used in our prior work and the references therein [10,65,68]. The price of Illinois Bituminous #6 coal is assumed to begin at \$45.0 tonnes^{-1} and be subjected to an inflation rate of 2.5% per year of operation. Overall, the base case cost estimates are meant to be as accurate as possible for the well-established technologies, but conservative for the up-and-coming technologies. A sample spreadsheet that itemizes the capital and operating costs for each of the plants examined is provided as Supplementary material.

Table 2
Description of simulated cases.

Case number	Tag	WGS enabled?	CAES enabled?	TSD enabled?	CCS enabled?
Pulverized Coal Systems					
1	SCPC	N/A	N/A	N/A	No
2	SCPC–CCS	N/A	N/A	N/A	Yes
SOFC Systems					
3	WGS	Yes	No	No	No
4	WGS–CCS	Yes	No	No	Yes
5	WGS–TSD	Yes	No	Yes	No
6	WGS–CCS–TSD	Yes	No	Yes	Yes
7	WGS–CAES	Yes	Yes	No	No
8	WGS–CCS–CAES	Yes	Yes	No	Yes
9	WGS-TSD-CAES	Yes	Yes	Yes	No
10	WGS–CCS–TSD–CAES	Yes	Yes	Yes	Yes
11	nWGS	No	No	No	No
12	nWGS–CCS	No	No	No	Yes
13	nWGS–TSD	No	No	Yes	No
14	nWGS–CCS–TSD	No	No	Yes	Yes
15	nWGS–CAES	No	Yes	No	No
16	nWGS–CCS–CAES	No	Yes	No	Yes
17	nWGS–TSD–CAES	No	Yes	Yes	No
18	nWGS–CCS–TSD–CAES	No	Yes	Yes	Yes

Table 3
Assumed parameters for case studies.

Parameter	Value	Units[a]
Initial price of coal	45.00	\$ tonnes^{-1}
HHV of coal	27,267	kJ kg^{-1}
CO_2 tax[b]	50.00	\$ tonnes^{-1}
Plant lifetime	20	Years
Discount rate	10.0	%
Inflation rate	2.5	%

[a] Cost units are expressed in US\$2007 using the Chemical Engineering Cost Index [62].
[b] This CO_2 tax is the "standard" for comparison, but is investigated in greater detail in Section 3.4.

3. Results and discussion

3.1. Overall system results and performance

3.1.1. Comparison of SCPC and SOFC processes

A summary of the operational results for each case investigated is presented below in Table 4. It is clear in this table that the SOFC systems, in general, behave differently than the traditional SCPC process. SOFC-based systems use less fuel that the SCPC plants, particularly in the cases where CCS is enabled. The base-load SOFC plant with WGS enabled, for example (case 3), uses 7% less coal (~150,000 tonnes per year) than the SCPC process. When CCS is enabled, the high parasitic energy costs associated with solvent-based CCS in the SCPC plant causes its fuel consumption to increase drastically in order to provide the same base load, whereas the SOFC–CCS (case 4) plant configuration is able to provide nearly the same amount of power without an increase in fuel consumption. When comparing cases 2 and 4, the fuel savings experienced by the SOFC base-load plant over its SCPC counterpart approaches 1,080,000 tonnes per year (35% savings). Furthermore, it can be seen that the direct CO_2 emissions from all of the SOFC plants with CCS are negligible, whereas they are still significant with the SCPC–CCS case due to the imperfect CO_2 recovery of the solvent-based CCS approach. It is also clear in Table 4 that all of the WGS-enabled SOFC processes (cases 3–10) have efficiencies 2.5–3.7 percentage points higher than the SCPC process, even with the inclusion of CAES and TSD (cases 7–10). When CCS is required, the SOFC-based systems are as much as 15 percentage points more efficient.

3.1.2. Effect of water–gas shift step

When comparing similar cases with and without the WGS step (cases 3–11, 4–12, etc.), it is clear that the overall efficiency of the plant decreases by approximately 3 percentage points. This lowered efficiency is mainly due to the decreased effectiveness of the SOFC stacks, caused by the presence of small amounts of H_2S in the cleaned fuel stream. The ideal potential of the SOFCs is more affected by H_2S in the presence of CO, leading to an overall lower efficiency of the SOFC stack, and therefore the entire plant. Furthermore, the CO oxidation reaction (Equation (2)) is more exothermic than the oxidation of H_2 (Equation (1)). Consequently, more energy from the fuel stream is lost to the surroundings through process inefficiencies as heat, and a greater degree of the chemical energy contained in the fuel stream is converted to thermal energy in the exhaust stream, instead of electricity. Although most of this additional heat is recovered in the HRSG, the lower overall efficiency of the HRSG compared to the SOFC stacks

Table 4
Overall and environmental system performance.

Case	1 SCPC	2 SCPC CCS	3 WGS	4 WGS CCS	5 WGS TSD	6 WGS CCS TSD	7 WGS CAES	8 WGS CCS CAES	9 WGS TSD CAES
Direct fuel usage (10^3 tonnes yr^{-1})	2137	3070	1988	1988	1799	1799	1988	1988	1799
Direct CO_2 emitted (10^3 tonnes yr^{-1})	5065	724.5	4463	0	4038	0	4463	0	4039
Indirect CO_2 emitted (10^3 tonnes yr^{-1})	48.99	48.99	40.48	48.99	85.02	102.4	14.51	20.56	54.25
Total CO_2 emitted (10^3 tonnes yr^{-1})	5114	773.5	4504	48.99	4124	102.4	4478	20.56	4093
CO_2 sequestered (10^3 tonnes yr^{-1})	0	7245	0	4463	0	4039	0	4463	0
Electricity generated (10^3 MW-h yr^{-1})	6300	6300	6422	6300	5809	5699	6345	6217	5640
Electricity sold (10^3 MW-h yr^{-1})	5390	5390	5411	5390	5301	5258	5474	5459	5377
Electrical efficiency[a] (%HHV)	39.1	28.4	42.9	42.0	42.8	42.0	42.3	41.5	41.6

Case	10 WGS–CCS TSD–CAES	11 nWGS	12 nWGS CCS	13 nWGS TSD	14 nWGS CCS TSD	15 nWGS CAES	16 nWGS CCS CAES	17 nWGS TSD CAES	18 nWGS–CCS TSD CAES
Direct fuel usage (10^3 tonnes yr^{-1})	1799	2175	2175	1969	1969	2175	2175	1969	1969
Direct CO_2 emitted (10^3 tonnes yr^{-1})	0	4939	0	4469	0	4939	0	4469	0
Indirect CO_2 emitted (10^3 tonnes yr^{-1})	76.05	39.60	48.99	83.21	102.4	13.35	19.75	30.35	45.69
Total CO_2 emitted (10^3 tonnes yr^{-1})	76.05	4979	48.99	4552	102.4	4952	19.75	4500	45.69
CO_2 sequestered (10^3 tonnes yr^{-1})	4039	0	4939	0	4469	0	4939	0	4469
Electricity generated (10^3 MW-h yr^{-1})	5509	6436	6300	5821	5699	6366	6226	5673	5551
Electricity Sold (10^3 MW-h yr^{-1})	5323	5413	5390	5305	5258	5477	5461	5435	5398
Electrical efficiency (%HHV)	40.6%	39.3%	38.4%	39.2%	38.41%	38.8%	38.0%	38.2%	37.4%

[a] Electrical efficiency is calculated as the total power generated by the plant divided by the total HHV fuel input to the plant on a basis of 1 year, whether or not that electricity was actually "sold" to the grid for profit.

lead to a decreased thermal efficiency of the plant overall. As such, in order to achieve comparable base-load plant outputs, the non-WGS cases require an overall higher fuel input to compensate for their lower efficiencies. Higher fuel consumption further causes as much as a 10% increase in the amount of carbon sequestered or emitted, causing increased operational costs. Whether or not the higher operating costs associated with omitting the WGS step outweigh the increased capital costs associated with its implementation in a purely economic sense is discussed in Section 3.2.

3.1.3. Effect of compressed air energy storage

As expected, the addition of CAES (cases 7–10 and 15–18) marginally decreases the overall thermal efficiency of the proposed system. This efficiency decrease is due to the higher losses associated with the CAES turbomachinery, as well as a less effective heat integration strategy due to an additional cooling/pre-heating step to/from 50 °C (recall it is assumed that the HRSG cannot recover energy in streams below 110 °C). However, these efficiency penalties are on the order of 1 percentage point, which is quite promising considering the significant practical value of peaking power which it enables. The improved peaking capabilities provided by the integrated CAES system significantly reduces the power that must be purchased from the grid over a one-year operating period. Consequently, the indirect CO_2 emissions for CAES-enabled plants are always lower than those of their non-CAES counterparts. This effect is even more prominent in the TSD cases, where the CAES system is utilized to a higher degree due to the seasonal shifts in base-load output. For example, when comparing cases 13 and 17 (See Table 4), case 13 requires approximately 177,000 MW-h less of purchased grid electricity, which corresponds to a decrease in CO_2 emissions of 53,000 tonnes (63.5%) over a one-year operating period. Finally, it should be noted that in scenarios when grid power is not available, the addition of CAES greatly improves reliability while also allowing for a much smaller base-load plant to be constructed.

3.1.4. Effect of train shutdown

As can be seen in Table 4, the addition of TSD to the SOFC-based systems has a negligible impact on the overall efficiency of the plant. However, adding TSD significantly reduces the amount of coal consumed due to its reduced operating level for several months of the year. For example, case 5 uses approximately 188,000 tonnes less of coal per year than case 3 (9.5%), which further leads to a proportional decrease in CO_2 emissions (when CCS is not implemented) or sequestration (when CCS is implemented). However, these decreases in fuel consumption and exiting CO_2 amounts come at the cost of meeting less consumer demand, leading to an increase in indirect CO_2 emissions stemming from grid electricity purchases. More detail regarding the effects of TSD on economics and load following are discussed in the proceeding sections.

3.2. Economic results

3.2.1. Comparison of SCPC and SOFC processes

Table 5 contains a summary of the economic data for each plant configuration examined in this work. Case 1 (SCPC) requires the

Table 5
Economic results for each of the plant configurations simulated.

Case	1 SCPC	2 SCPC CCS	3 WGS	4 WGS CCS	5 WGS TSD	6 WGS CCS TSD	7 WGS CAES	8 WGS CCS CAES	9 WGS TSD CAES
Capital cost ($1,000,000s)	1015	1849	1835	1873	1835	1873	2059	2097	2059
Grid power cost ($1000s yr^{-1})	5456	5456	4598	5456	8741	10,346	1762	2460	5159
Fuel costs ($1000s yr^{-1})	96,140	138,170	89,470	89,470	80,960	80,960	89,470	89,470	80,960
CO_2 Emission costs[c,d] ($1000s yr^{-1})	255,700	56,790	225,200	13,610	206,200	15,220	223,900	12,190	204,600
Operating costs[a] ($1000s yr^{-1})	39,700	85,270	60,960	72,110	60,680	70,780	60,960	73,870	62,430
LCOE[b] (¢ kW^{-1} h^{-1})	5.35	9.12	7.42	7.80	7.47	7.88	7.78	8.15	7.81
LCOE[c] with CO_2 tax (¢ kW^{-1} h^{-1})	11.04	9.98	12.40	7.85	12.13	7.99	12.69	8.17	12.36

Case	10 WGS–CCS TSD CAES	11 nWGS	12 nWGS CCS	13 nWGS TSD	14 nWGS CCS TSD	15 nWGS CAES	16 nWGS CCS CAES	17 nWGS TSD CAES	18 nWGS–CCS TSD CAES
Capital cost ($1,000,000s)	2097	1861	1901	1861	1901	2090	2130	2090	2130
Grid power cost ($1000s yr^{-1})	6877	4506	5456	8571	10,346	1635	2374	3537	5114
Fuel costs ($1000s yr^{-1})	80,960	97,900	97,900	88,580	88,580	97,900	97,900	88,580	88,580
CO_2 emission costs[c,d] ($1000s yr^{-1})	13,900	248,900	14,800	227,600	16,290	247,600	13,340	225,000	13,460
Operating costs[a] ($1000s yr^{-1})	72,530	61,220	73,570	60,930	72,100	62,970	75,320	62,680	73,850
LCOE[b] (¢ kW^{-1} h^{-1})	8.24	7.66	8.08	7.69	8.14	8.04	8.43	7.93	8.36
LCOE[c] with CO_2 tax (¢ kW^{-1} h^{-1})	8.32	13.17	8.13	12.83	8.26	13.45	8.46	12.89	8.41

[a] Operating costs include labour, maintenance, catalysts, water consumption, CO_2 transport costs, and materials.
[b] Does not include a CO_2 tax.
[c] Includes a CO_2 tax of $50 tonnes^{-1}.
[d] Includes sequestration costs of $2.5 tonnes^{-1}.

lowest total capital investment due to its high maturity and proven technology when compared to any of the SOFC-based cases. In fact, the SCPC plant costs at least $860 million less than any of the SOFC cases when CCS is not required. However, case 2 indicates that the addition of CCS to the SCPC plant would bring its capital costs up significantly, approaching the costs of an SOFC system while at the same time greatly increasing fuel requirements (due to the much lower efficiency resulting from CCS addition). Although the fuel costs for case 1 are higher than most of the SOFC cases (some non-WGS cases are less efficient overall than the SCPC plant), the increase in fuel costs is overshadowed by its lower capital and operating costs. The resulting LCOE for the SCPC case is 5.35 ¢ kW^{-1} h^{-1} and is the lowest among all cases when no CO_2 tax is implemented and CCS is not required. However, when a CO_2 tax of $50 tonnes^{-1} is implemented it is clear that the high CO_2 emissions from the SCPC plant cause a significant increase in annual operating costs leading to an unattractive LCOE of 11.04 ¢ kW^{-1} h^{-1} (an increase of 106%). Even when CCS is added to the SCPC plant under a CO_2 taxed scenario, case 2 remains the most expensive option of any CCS-enabled processes investigated. In fact, case 2 has the highest LCOE among all cases examined when no CO_2 emission penalty is included.

3.2.2. Effect of water–gas shift step

When comparing any of the WGS-enabled processes to their non-WGS counterparts, it can be seen in Table 5 that the capital and operating costs for non-WGS cases are actually higher, leading to an increase in LCOE. The increased capital costs stem from the fact that since the non-WGS cases operate at a lower efficiency, the plant must be scaled up (using a higher fuel throughput as discussed in Section 3.1.2) to reach the required base-load output of 719 MW. Consequently, nearly all of the major process units must be scaled up to accommodate this throughput increase. The resulting added capital costs from scale-up slightly outweigh the cost of the WGS reactors themselves, leading to a modest (1–2%) increase in total capital investment. As a result, the higher capital and operating costs of the non-WGS cases lead to higher results for the LCOE metric, regardless of the design decisions. For example, when comparing cases 7 (WGS–CAES) and 15 (nWGS–CAES) in the absence of a CO_2 tax, case 15 has a $30 million higher capital cost and requires an additional $10.5 million per year in total operating and fuel costs, leading to a 3.2% higher LCOE (8.04 ¢ kW^{-1} h^{-1} versus 7.79 ¢ kW^{-1} h^{-1}). It can therefore be concluded from this investigation that the inclusion of a WGS step will decrease the total lifetime cost of the proposed SOFC/CAES plant, bearing in mind that these results are strongly dependant on the value of the ideal voltage when H_2S is in the presence of CO (see Section 2.2.4). It should further be mentioned that the assumed SOFC stack cost of $1000 kW^{-1} was maintained through each plant configuration. In the cases where WGS was not included, the SOFC electrical output decreased significantly, leading to a lower stack cost in the non-WGS cases. Should a constant physical stack size (and therefore cost) have been assumed, the capital cost for the non-WGS cases would have been even higher, further increasing their values for LCOE and motivating the inclusion of WGS.

3.2.3. Effect of compressed air energy storage

As expected, the addition of CAES to the SOFC base-load plant increases capital costs due to the additional turbomachinery and storage investments (see Table 5). However, the addition of CAES offers some decreases in the amount of supplementary grid power that must be purchased and costs associated with indirect CO_2 emissions. Comparing cases 4 and 8, it is clear that the addition of CAES results in a ~$225 million (12%) increase in capital costs. This increase is constant throughout all cases utilizing CAES since the turbomachinery and cavern sizes are all the same. However, the

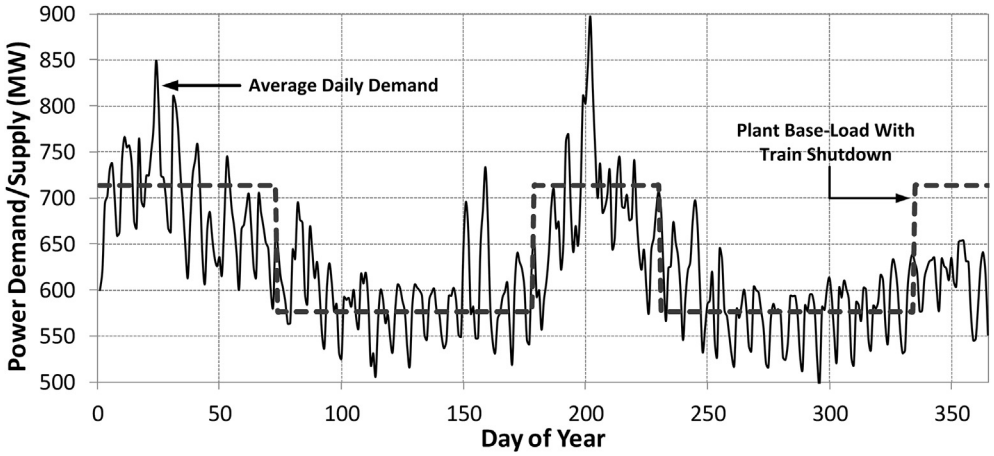

Fig. 5. Average daily demand and base-load plant train shutdown schedule for one simulated year of operation. Reproduced from Ref. [10].

annual amount of grid power that must be purchased decreases by ~$3 million per year (55%) when CAES is enabled. Furthermore, since the CAES-enabled plant in case 8 incurs 28,500 (58%) tonnes per year less indirect CO_2 emissions, it saves an additional $1.5 million per year in CO_2 taxes (assuming $50 tonnes^{-1}). When these effects are combined, the inclusion of CAES can be seen to cause a modest increase in a plant's LCOE of ~0.3 ¢ kW^{-1} h^{-1} or 0.35 ¢ kW^{-1} h^{-1} with or without a CO_2 tax of $50 tonnes^{-1}, respectively. Therefore, with a 3–4% increase in overall electricity costs, the addition of CAES can greatly improve reliability and grid independence. Finally, it is important to mention that if the assumed plant lifetime for this analysis were to increase, the decreased annual operating costs associated with adding CAES would further reduce its relative LCOE to a strictly base-load plant configuration.

3.2.4. Effect of train shutdown

It is clear in Table 5 that the inclusion of TSD has no effect on capital cost. Furthermore, cases with TSD have lower operating and significantly lower fuel costs than their constant base-load counterparts. For example, case 14 uses 9.5% less coal (equating to ~$9.3 million year^{-1}) than case 12. However, TSD significantly increases the amount of grid electricity that must be purchased and the indirect CO_2 emissions associated with it. Case 14 requires almost $5 million year^{-1} more in grid electricity purchases when compares to case 12, corresponding to a 90% increase. Furthermore, the TSD cases are able to sell less electricity by meeting less demand; even though the overall annual operating and fuel costs is lower for cases using TSD, the smaller amount of useable electricity produced results in a slightly higher LCOE. As expected, this gap increases when a CO_2 tax is implemented. Through the combination of TSD and CAES, both fuel savings and reduced dependence on grid electricity (and all associated indirect emissions) is possible but at higher capital cost, essentially providing a hybrid "best of both worlds" scenario.

3.3. Load-following results and performance

A sample plot of demand and power provided by case 8 (WGS–CCS–CAES) is given in Fig. 6, and the corresponding cavern pressure profile is displayed in Fig. 7. Table 6 summarizes the load-following results for each case. The CAES-enabled system is clearly able to follow demand fluctuations above and below the base-load output of the SOFC and HRSG together (the WGS–CCS case) with a high degree of reliability during most of the simulated control intervals.

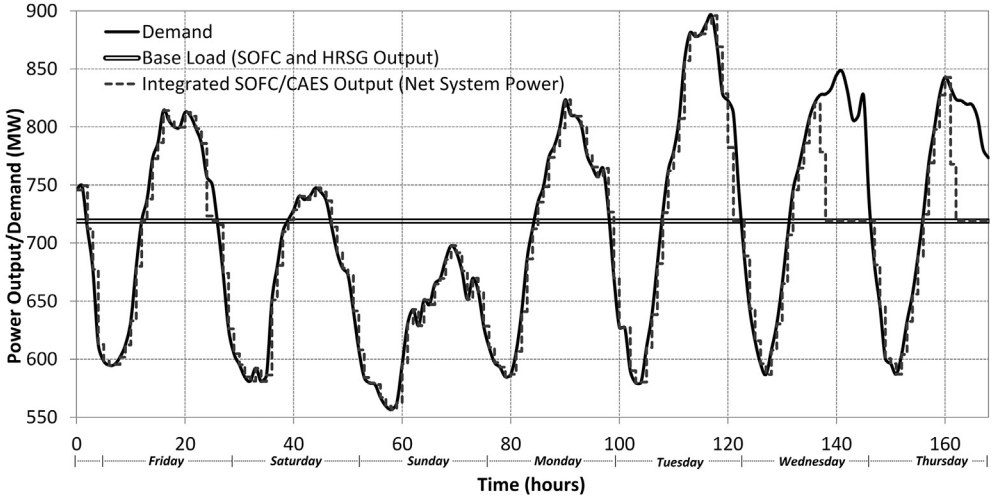

Fig. 6. Simulation results of the SOFC/CAES system for one selected week of operation (June 17–23, 2011). Times in which the output of the SOFC/CAES system matches the base load when demand is less than supply denote times when the cavern is full (at maximum allowable pressure). Times in which the SOFC/CAES system matches the base load when demand exceeds supply denote times when the storage cavern is empty (at minimum allowable pressure).

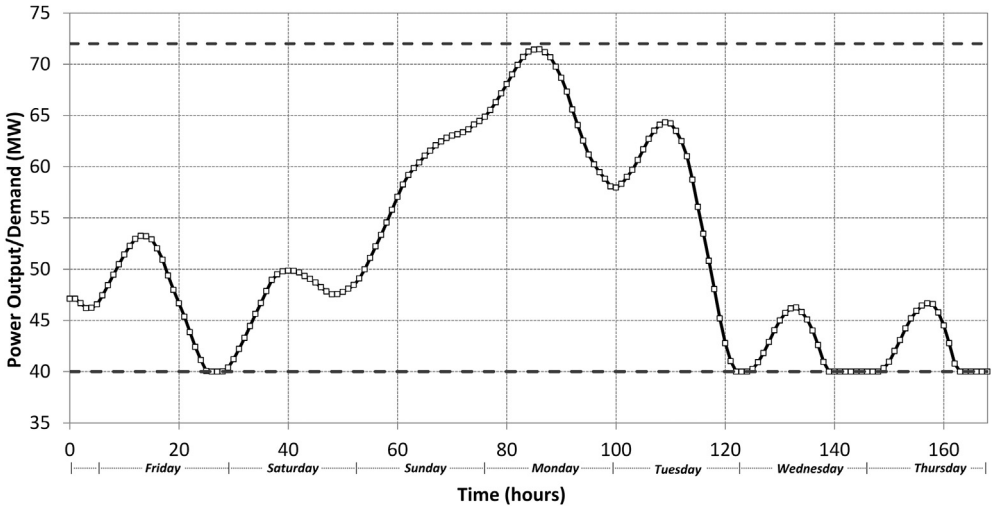

Fig. 7. Pressure profile for one week of simulated operation (June 17–23, 2011).

As reported in Table 6, the addition of CAES to any of the SOFC base-load configurations significantly improves the SSE and WSEE. For example, when comparing case 9 (WGS–CCS–CAES) to case 4 (WGS–CCS), the SSE and WSSE metrics decrease by 42.6% and 38.6%, respectively. Adding TSD also reduces the SSE and WSSE metrics when compared to a standard base-load SOFC plant due to a lower total demand/supply mismatch (this trend is evident in Fig. 5). However, the improvement in WSSE is less significant when TSD is added due to its higher weighting on the under-production of demand. For example, case 5 has a SSE less than 50% of that of case 3 due to the addition of TSD, but the WSSE is reduced by only 29%. Utilizing both CAES and TSD results in the best load following performance because the CAES system is able to minimize the amount of underproduction that arises due to the introduction of TSD. Interestingly, case 18 (nWGS–CCS–TSD–CAES) has the lowest overall SSE and WSSE. Since the SOFC stacks are inherently less efficient in the non-WGS cases, the reduction in base-load output is less significant when TSD is used. Consequently, the ability of the plant (while using TSD) to meet demand using the CAES system is improved, resulting in better load-following during those times.

Table 6
Load-following metric results for cases investigated.

Case	Tag	SSE (10^6 [MW-h]^2)	WSSE (10^6 [MW-h]^2)	Relative SSE	Relative WSSE
1	SCPC	162.6	51.8	0.86	0.93
2	SCPC–CCS	162.6	51.8	0.86	0.93
3	WGS	186.3	55.5	0.98	0.99
4	WGS–CCS	162.6	51.8	0.86	0.93
5	WGS–TSD	88.2	39.1	0.47	0.70
6	WGS–CCS–TSD	81.7	41.8	0.43	0.75
7	WGS–CAES	159.5	44.4	0.84	0.79
8	WGS–CCS–CAES	134.6	40.0	0.71	0.71
9	WGS–TSD–CAES	50.7	24.1	0.27	0.43
10	WGS–CCS–TSD–CAES	45.5	27.7	0.24	0.50
11	nWGS	189.1	55.9	1.00	1.00
12	nWGS–CCS	162.6	51.8	0.86	0.93
13	nWGS–TSD	89.0	38.9	0.47	0.70
14	nWGS–CCS–TSD	81.7	41.8	0.43	0.75
15	nWGS–CAES	163.2	45.0	0.86	0.80
16	nWGS–CCS–CAES	135.4	40.0	0.72	0.71
17	nWGS–TSD–CAES	45.68	20.06	0.24	0.36
18	nWGS–CCS–TSD–CAES	38.63	22.33	0.20	0.40

Given in Fig. 8 is a two-dimensional map that shows the relative positioning of each process investigated in terms of load-following and economic performance. System configurations toward the lower-left corner of Fig. 9 are those with the best LCOE and SSE results. It can be seen that cases using CCS, CAES and TSD offer the best load-following performance while also remaining economically superior or competitive with other configurations. In particular, case 10 offers the best LCOE/SSE trade-off while also being almost unaffected by the implementation of a \$50 tonnes^{-1} CO_2 tax.

3.4. Sensitivity of carbon tax on plant economics

The LCOEs for each of the cases examined computed as a function of the average lifetime carbon tax paid by the plant and are shown in Fig. 8. Note that the cases without a WGS step have essentially the same slopes as their WGS-enabled counterparts with only a small offset, and so for the sake of clarity are omitted from Fig. 8. This analysis assumes a simple linear CO_2 tax on a per-tonne basis. With the price of coal at \$45 tonnes^{-1}, it would require a CO_2 tax of \$22 tonnes^{-1} to incentivize a system in which CCS is used (noting that it is one of the SOFC designs); anything less would make CCS uneconomical compared to the non-CCS cases. Furthermore, it can be seen in Fig. 8 that once CCS is economically advantageous, only SOFC base-load plants with CCS are competitive. This analysis also confirms that the CAES system at no point becomes more economical than any of its non-CAES counterparts. This is not surprising, since added flexibility and reliability does not come without a cost, and no economic incentive for flexibility was included in this analysis. However, the added cost of a CAES system is small to the end consumer (0.35 ¢ kW^{-1} h^{-1}), and may become even more favourable if it is combined with current electricity price estimates and an economic optimization objective, which is left to future work. The closeness of the SOFC-based cases without a CO_2 tax owes to the very low cost of adding the CCS method described in Section 2.2.5. One of the strongest aspects of the SOFC/CAES system proposed in this work is that CCS may be retro-fitted to an already existing base-load plant with minimal process alterations, making it an excellent forward-looking insurance policy against future CO_2 emission regulations. Finally, this analysis indicates that SCPC with solvent-based CCS becomes economically advantageous compared to a SCPC process at a CO_2 tax of \$38 tonnes^{-1}, but is inferior to the SOFC-based systems at all CO_2 tax levels.

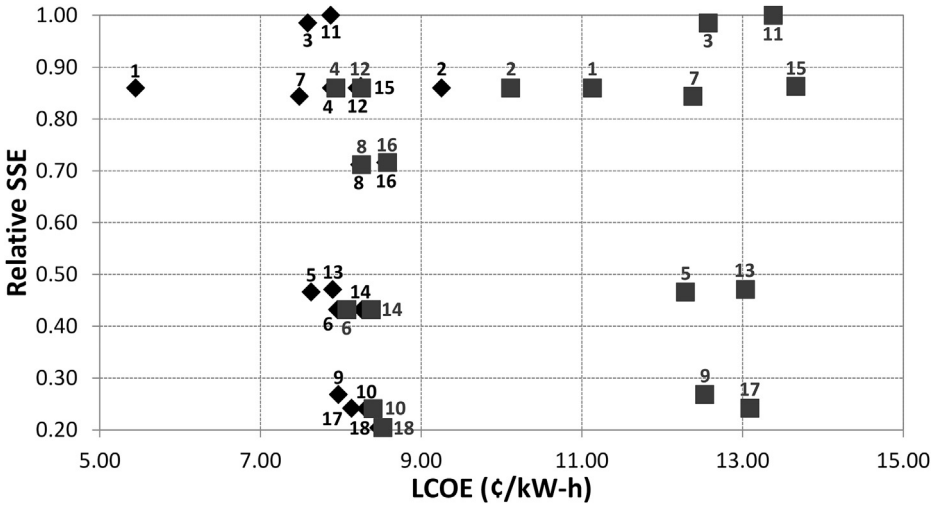

Fig. 8. Map of LCOE (economic indicator) versus SSE (load-following indicator) with (grey squares) and without (black diamonds) a \$50 tonnes^{-1} CO_2 tax. Each symbol is labelled with its corresponding case number as defined in Table 2.

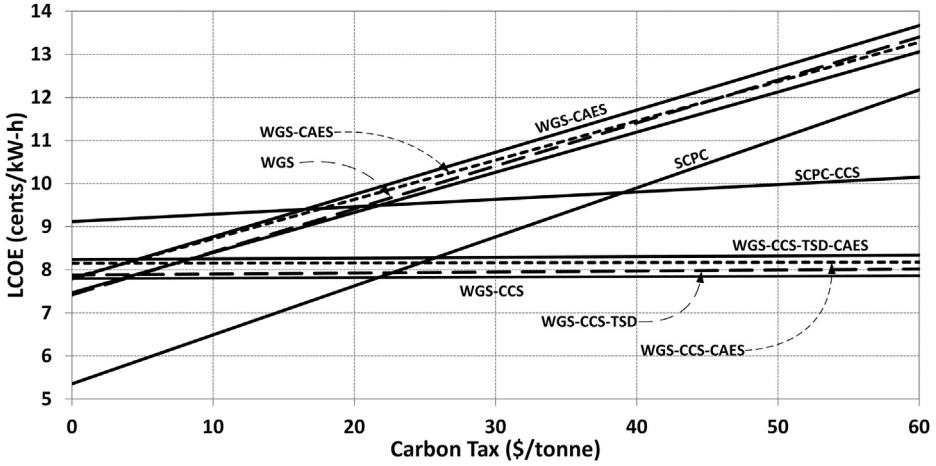

Fig. 9. Effect of CO_2 taxes on LCOE (WGS and SCPC cases).

3.5. Sensitivity analyses of assumed economic parameters

In order to assess the impacts of the assumptions made for this analysis, a comprehensive sensitivity analysis of the most uncertain variables was performed. Because of the high number of configurations investigated in this study, a candidate case was chosen to be the subject of the sensitivity analysis when analyzing the impact of the assumed parameters on LCOE (Section 3.5.1). To this end, case 10 (SOFC with WGS, CAES, CCS and TSD as described in Table 2) was chosen because it includes all of the possible design options and thus would be affected by all of the perturbed variables. A summary

Table 7
Variables and bounds for the sensitivity analysis.

Perturbed variable	Base case	Lowest value	Highest value	% Change (+/−)
CAES capital cost (\$ Thousands)	201,558	151,168	251,948	25
Discount rate (%)	10.0	7.5	12.5	25
SOFC stack cost (per kW)	500	300	700	40
Initial price of coal (\$ tonnes^{-1})	45	30	60	33
Plant lifetime[a] (years)	20	15	25	25
SOFC stack lifetime[a] (years)	10	8	12	20
Inflation rate (%)	2.5	1.5	3.5	40
CO_2 sequestration cost (\$ [tonne sequestered]$^{-1}$)	2.50	0	5.00	100

[a] Represents a variable where the higher value is a favourable case. All other variables are favourable when they are lowered.

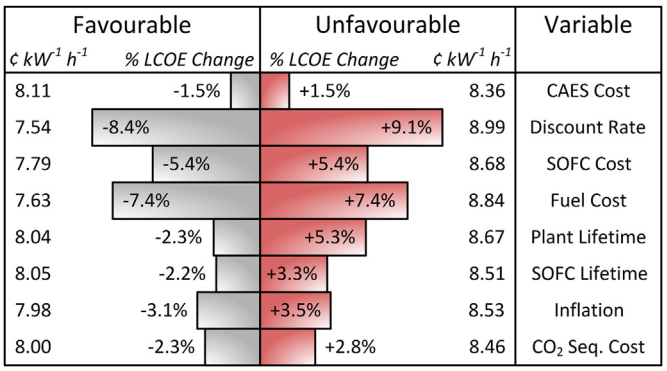

Fig. 10. Effect of sensitivity variables on the LCOE of the SOFC–WGS–CCS–CAES–TSD case.

of the variables that were altered for the sensitivity analysis is shown in Table 7, and a CO_2 tax of \$50 tonnes^{-1} was assumed for this sensitivity analysis.

A second sensitivity analysis was performed to specifically determine the effect on the breakeven CO_2 price (Section 3.5.2). In this analysis, the variables are altered in the same way (Table 7) as in the first sensitivity analysis, except that a constant CO_2 tax is no longer assumed. Instead, the CO_2 tax in which the SOFC-based plant becomes more economically favourable than the SCPC process is reported. A sensitivity analysis was not performed on the NETL pulverized coal plant cost estimates.

3.5.1. Effect of economic assumptions on LCOE of SOFC–CAES plant with CCS

The *Ceteris Paribus* ("all else being equal") sensitivity results that show the impact each of the main assumptions made in Table 7 have on the LCOE of the candidate plant are summarized in Fig. 10. It can be seen that the assumed discount rate (originally assumed to be 10%) has the largest effect on the LCOE of the candidate case. Increasing the discount rate by 2.5 percentage points (25%) increases the LCOE by 9.1% to almost 9 ¢ kW^{-1} h^{-1}. Moreover, the cost of coal has a large impact on the economics of the candidate case, changing the LCOE by ±7.4% (0.61 ¢ kW^{-1} h^{-1}) with a change of ±33% (\$15 tonnes^{-1}). Another interesting feature of Fig. 10 is that the capital cost of the CAES system does not have a large impact on plant economics. A 25% change in the cost of capital for the CAES system results in only a 1.5% change in LCOE. This means two things: a) the development of a SOFC/CAES plant is robust to uncertainties around the price of the CAES system, and b) a CAES can be retro-fitted on to an existing SOFC plant with a minimal impact on LCOE should peaking power be required. Finally, it is clear that LCOE is also strongly dependant on the SOFC stack cost (as it represents the largest capital expenditure), the lifetime of the plant, and the lifetime of the individual SOFC stacks (thereby requiring more frequent replacements). However, for all perturbations considered, the LCOE of the candidate case remains below that of SCPC (11 ¢ kW^{-1} h^{-1}) and SCPC–CCS (10 ¢ kW^{-1} h^{-1}) with a CO_2 tax of \$50 tonnes^{-1}.

3.5.2. Effect of economic assumptions on breakeven CO_2 tax

The sensitivity results that show the impact of the assumed economic parameters listed in Table 7 on the breakeven CO_2 tax (the point at which the SOFC plants become economically favourable over the current SCPC process) are shown in Fig. 11.

It can be seen that the SOFC stack cost and discount rate both have a large impact on the breakeven price of CO_2. Increasing the SOFC stack cost by \$300 kW^{-1} (30%) leads to an increase of \$3.6 tonnes^{-1} (16.4%) in the breakeven price of CO_2. This is not surprising, since the SOFC stack represents the majority of the plant cost and the main source of economic benefit for any of the SOFC-based plants compared to the SCPC plants is the avoidance of a potential CO_2 tax. Moreover, decreasing the SOFC stack cost by \$300 kW^{-1} (30%) leads to a \$4.4 (20%) tonnes^{-1} decrease in the breakeven price of CO_2. Perturbations of ±2.5 percentage points (25%) to the discount rate lead to changes in the breakeven CO_2 price of \$3.1 tonnes^{-1} (14%, unfavourable) and −\$2.75 tonnes^{-1} (12.5%, favourable), respectively. This is due to the large impact that the discount rate demanded by investors has on the capital investment, which is much higher for the SOFC cases than the SCPC cases. It is interesting to note that the CAES cost does not have an impact on the breakeven price of CO_2 in this scenario. This is because the plant configurations using CAES have a consistent (although small) price premium for the flexibility that the CAES system adds. Finally, it is interesting that the CO_2 sequestration cost has a much larger impact on the breakeven CO_2 price than the overall LCOE as discussed in section 3.5.1. An increase of \$2.5 tonnes^{-1} (100%) in the sequestration price increases the breakeven price of CO_2 by \$1.9 tonnes^{-1} (8.6%), whereas it only had a 2.8% impact on the LCOE. An increase in the sequestration cost of CO_2 has a direct impact on the potential net savings of CO_2 sequestration, which therefore leads to a significant impact on the required CO_2 tax to justify its use.

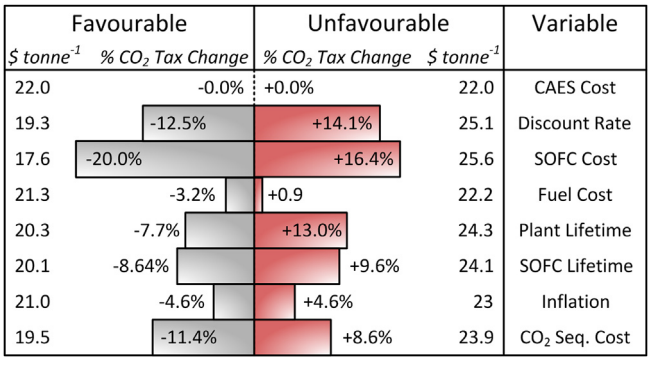

Fig. 11. Effect of sensitivity variables on the breakeven CO_2 tax.

4. Conclusions and future work

In this study, a novel integrated coal-fuelled SOFC/CAES system with and without optional WGS and CCS steps was investigated. Sixteen different SOFC plant configurations were simulated using a combination of Aspen Plus and MATLAB simulation tools (in-house models) and were compared to industrially standard SCPC processes. It was found that the addition of CAES to an SOFC-based system significantly improves load-following capabilities with minimal increases to LCOE (<0.3 ¢ kW^{-1} h^{-1}). Adding CAES significantly improved the load-following metrics (SSE and WSSE) of the proposed system, and was not negatively affected by the inclusion of CCS. Furthermore, the inclusion of CCS was able to reduce the total CO_2 emissions of the plant to nearly zero with a marginal increase in capital cost and no losses to overall plant operability. The inclusion of TSD was found to further improve the load-following capabilities of a CAES-enabled plant while also providing fuel savings and fuel cell maintenance windows. The addition of the WGS was found in this study to improve the overall economic performance of the plant due to the reduced electrical efficiency of the SOFC stacks when the fuel gas contains a combination of CO and H_2S. This resulted in higher capital costs, but reduced fuel and operating costs throughout the lifetime of the plant.

Overall, the SOFC/CAES process, when utilizing CCS and WGS, is capable of providing reliable load-following with zero direct (and nearly zero indirect) CO_2 emissions with only a marginal increase to LCOE. Furthermore, the SOFC-based systems with CCS become the most economically attractive option when CO_2 taxes of ~\$22 tonnes^{-1} or higher are considered. Sensitivity analyses show that the economic results for the SOFC-based plants depend on some key assumptions (listed in Table 7), but still consistently show improvement over the current state-of-the-art when CO_2 taxes are considered. Although SOFCs may be years away from being implemented at the bulk-generation scale, the forward-looking power production strategies proposed in this work show promise for providing clean and reliable peaking power in the future.

To the best of our knowledge, the investigation of peaking power generation from coal has not been explored yet. As a result, several simplifying assumptions were made in this study in order to provide a proof-of-concept framework. Future work may look at

dynamics associated with turbines, compressors and the HRSG and their effect on load-following capabilities. Furthermore, real-time optimization can be used with future predictions of demand to optimize the profitability or load-following capabilities of the SOFC/CAES system, potentially including stochastic fuel and electricity pricing, startup/shutdown penalties of using TSD, or considering CO_2 to have economic value. Different (potentially renewable) fuel sources may also be investigated, such as biomass and petroleum coke.

Nomenclature

Abbreviations

ASU	air separation unit
CAES	compressed air Energy storage
CCS	carbon capture and sequestration
EOS	equation of state
HHV	higher-heating value
HRSG	heat recovery and steam generation
LCOE	levelized cost of electricity
NGCC	natural gas combined cycle
SOFC	solid oxide fuel cell
SSE	sum of squared error
TSD	train shutdown
WGS	water–gas shift
WSSE	weighted sum of squared error
SCPC	supercritical pulverized coal
nWGS	no water–gas shift reactors

Mathematical symbols

D	demand
F	fuel costs
I	capital investment
M	maintenance costs
N	plant lifetime
O	plant over-production
P	sellable power produced
r	discount rate
U	plant under-production

Appendix A. Supplementary data

Supplementary data related to this article can be found at http://dx.doi.org/10.1016/j.jpowsour.2013.11.040.

References

[1] US Energy Information Administration, AEO2012 Early Release Outlook, US DOE/EIA-0383ER(2012), January 2012.
[2] National Energy Board. Canada's Energy Future: Energy Supply and Demand Projections to 2035 – Electricity Outlook Highlights, Available online: http://www.neb-one.gc.ca/clf-nsi/rnrgynfmtn/nrgyrprt/nrgyftr/2011/nrgsppldmndprjctn2035-eng.pdf (accessed June, 2012).
[3] H.J. Herzog, D. Golomb, in: C.J. Cleveland (Ed.), Encyclopedia of Energy, Elsevier Science, New York, 2004, pp. 277–287.
[4] A.J. Minchener, J.T. McMullan, J Energy Inst. 81 (2008) 38–44.
[5] Energy Information Administration (EIA), Fuel Emission Factors, Appendix H of Instructions to Form EIA-1605, U.S. Department of Energy, Washington, D.C., Available online: http://www.eia.gov/oiaf/1605/pdf/Form%20EIA-1605%20instructions.pdf.
[6] U.S. Environmental Protection Agency (EPA), Inventory of U.S. Greenhouse Gas Emissions and Sinks: 1990–2010, EPA 430-R-12–001, pp. 3–5, Available online:http://www.epa.gov/climatechange/ghgemissions/usinventoryreport.html.
[7] M.C. Woods, P.J. Capicotto, J.L. Haslbeck, N.J. Kuehn, M. Matuszewski, L.L. Pinkerton, M.D. Rutkowski, R.L. Schoff, V. Vaysman, Cost and Performance Baseline for Fossil Energy Plants. Volume 1: Bituminous Coal and Natural Gas to Electricity, August 2007. Final Report, DOE/NETL-2007/1281, Revision 1.
[8] M. Hasan, R. Baliban, J. Elia, C. Floudas, Ind. Eng. Chem. Res. 51 (2012) 15665–15682.
[9] M. Hasan, R. Baliban, J. Elia, C. Floudas, Ind. Eng. Chem. Res. 51 (2012) 15642–15664.
[10] J. Nease, T.A. Adams II, J. Power Sources 228 (2013) 281–293.
[11] M.C. Williams, J.P. Strakey, W.A. Surdoval, Int. J. Appl. Ceram. Technol. 2 (2005) 295.
[12] T.A. Trabold, J.S. Lylak, M.R. Walluk, J.F. Lin, D.R. Trojani, Int. J. Hydrogen Energy 37 (2012) 5190.
[13] T.A. Adams II, J. Nease, D. Tucker, P. Barton, Ind. Eng. Chem. Res. 52 (2013) 3089–3111.
[14] N.Q. Ming, ECS Trans. 7 (2007) 45.
[15] F.P. Nagel, T.J. Schildhauer, S.M.A. Biollaz, Int. J. Hydrogen Energy 34 (2009) 6809.
[16] H. Jin, E.D. Larson, F.E. Celik, Biofuels Bioprod. Bioref. 3 (2009) 142.
[17] T.A. Adams II, P.I. Barton, Systems and Methods for the Separation of Carbon Dioxide from Water, 2009, US Patent App. 12/434486.
[18] T.A. Adams II, P.I. Barton, AIChE J. 56 (2010) 3120–3136.
[19] T.A. Adams II, P.I. Barton, Fuel Proc. Technol. 92 (2011) 2105.
[20] P. Kuchonthara, S. Bhattacharya, A. Tsutsumi, Fuel 84 (2005) 1019–1021.
[21] A. Verma, A.D. Rao, G. Samuelsen, J. Power Sources 158 (2006) 417–427.
[22] M. Li, A. Rao, J. Brouwer, G. Samuelsen, J. Power Sources 195 (2010) 5707–5718.
[23] S. Park, J. Ahn, T. Kim, Appl. Energy 88 (2011) 2976–2987.
[24] E. Achenbach, J. Power Sources 57 (1995) 105–109.
[25] C. Stiller, B. Thorund, O. Bolland, J. Eng. Gas Turbines Power 128 (2006) 551–559.
[26] G. Almutairi, K. Kendall, W. Bujalski, Int. J Low-Carbon Technol. 7 (2012) 63–68.
[27] L. Barelli, G. Bidini, A. Ottoviano, Int J. Hydrogen Energy 37 (2012) 16140–16150.
[28] M. Raju, S.K. Khaitan, Appl. Energy 89 (2012) 474–481.
[29] E. Fertig, J. Apt, Energy Policy 39 (2009) 2330–2342.
[30] Dressler-Rand, Dresser-Rand Awarded Compressed Air Energy Storage (CAES) Project [press release], 2013. Available online: http://investor.dresser-rand.com/releasedetail.cfm?ReleaseID= 774720.
[31] L. Copelin, As Texas Worries about Power Generation, Is Answer Underground?, Statesman, April, 2013. Available online: http://www.statesman.com/news/business/as-texas-worries-about-power-generation-is-answe-1/nRmpY/.
[32] H. Hoffeins, Huntorf Air Storage Gas Turbine Power Plant, in: Energy Supply, Brown Boveri Publication, 1994. DGK 90 202 E.
[33] D.R. Hounslow, W. Grindley, R.M. Louglin, J. Eng. Gas Turbines Power 120 (1988) 875–883.
[34] A. Cavallo, Energy 32 (2007) 120–127.
[35] J.B. Greenblatt, S. Succar, D.C. Denkenberger, R.H. Williams, R.H. Socolow, Energy Policy 35 (2007) 1472–1492.
[36] J. Mason, V. Fthenakis, K. Zweibel, T. Hansen, T. Nikolakakis, Prog. Photovolt. Res. Appl. 16 (8) (2008) 649–668.
[37] S. Succar, R.H. Williams, Compressed Air Energy Storage: Theory, Resources and Applications for Wind Power, Princeton Environmental Institute: Princeton University, 2008.
[38] T.A. Adams II, P. Barton, J. Power Sources 195 (2010) 1971–1983.
[39] Independent Electricity System Operator, Ontario Demand and Market Prices, Available HTTP: http://www.ieso.ca/imoweb/siteShared/demand_price.asp?sid =ic (accessed 19.03.12).
[40] T.S. Lee, J.N. Chung, Y. Chen, Energy Convers. Manag. 52 (2011) 3214–3226.
[41] F. Mueller, B. Tarroja, J. Maclay, F. Jabbari, J. Brouwer, S. Samuelson, J. Fuel Cell Sci. Technol. 7 (2010) 031007-1–031007-12.
[42] L. Yang, Y. Weng, J. Power Sources 196 (2011) 3824–3835.
[43] V. Liso, A. Oleson, M. Nielson, S. Kaer, Energy 35 (2011) 4216–4226.
[44] Y. Komatsu, S. Kimijima, J.S. Szmyd, Energy 35 (2010) 982–988.
[45] T. Kuramochi, W. Turkenburg, A. Faaij, Fuel 90 (2011) 958–973.
[46] K. Krulla, in: SECA Conference Proceeding, United States Department of Energy – National Energy Technology Laboratory, Pittsburgh, PA, July 23–24, 2013.
[47] GREET, The Greenhouse Gases, Regulated Emissions, and Energy Use in Transportation Model, GREET 1.8d.1, Developed by Argonne National Laboratory, Argonne, IL, released, August 26, 2010. Available HTTP:, http://greet.es.anl.gov/.
[48] Aspen Technology, Inc., Aspen Plus User Guide, Version 2006.5, Software Documentation, Aspen Technology, Inc., Burlington, MA, 2006.
[49] J.P. Trembly, R.S. Gemmen, D.J. Bayless, J Power Sources 169 (2007) 347–354.
[50] K. Haga, S. Adachi, Y. Shiratori, K. Itoh, K. Sasaki, Solid State Ionics 179 (2008) 1427–1431.
[51] K. Sasaki, K. Susuki, A. Iyoshi, M. Uchimura, N. Imamura, H. Kusaba, Y. Teraoka, H. Fuchino, K. Tsujimoto, Y. Uchida, N. Jingo, J. Electrochem. Soc. 153 (2006) A2023–A2029.
[52] T.A. Adams II, P.I. Barton, J. Power Sources 195 (2010) 5152–5153.
[53] K. Lobachyov, J.H. Richter, J. Energy Resour. Technol. 118 (1996) 285–292.
[54] A.I. Marquez, T.R. Ohrn, J.P. Trembly, D.C. Ingram, D.J. Bayless, J Power Sources 164 (2007) 659–667.
[55] EG&G Technical Services, DOE/NETL Fuel Cell Handbook, seventh ed., November 2004.
[56] E. deVisser, C. Hendriks, M. Barrio, M.J. Mølnvik, G. de Koeijer, S. Liljemark, Y.L. Gallo, Int. J. Greenhouse Gas Control 2 (2008) 478–484.
[57] W.L. Luyben, Ind. Eng. Chem. Res. 50 (2011) 13984–13989.

[58] R. Kushnir, Transp. Porous Media 73 (2008) 1–20.
[59] Electric Power Research Institute, Wind Power Integration Technology Assessment and Case Studies, 2004. EPRI Report 1004806.
[61] K. Branker, M.J.M. Pathak, J.M. Pearce, Renew. Sustain. Energy Rev. 12 (2011) 4470–4482.
[62] D. Lozowski, Chem. Eng. 119 (2012) 80.
[63] H.C. Mantripragada, E.S. Rubin, Int. J. Greenhouse Gas Control 16 (2013) 50–60.
[64] R.D. Middleton, J.K. Eccles, Appl. Energy 108 (2013) 66–73.
[65] W.D. Seider, J.D. Seader, D.R. Lewin, S. Widago, Product and Process Design Principles, third ed., Wiley, Hoboken, NJ, 2009, pp. 534–597.
[66] G. Hossein, in: SECA Conference Proceeding, FuelCell Energy, Inc., Pittsburgh, PA, July 24–25, 2012.
[67] The Washington Post, At Redox Power Systems, the Future of Electricity Lies in Fuel Cells, 2013. Available online: http://articles.washingtonpost.com/2013-08-25/business/41446704_1_fuel-cells-warren-citrin-wind-power.
[68] R. Schainker, Compressed Air Energy Storage Cost Analysis, The Electric Power Research Institute, 2009. Report 1016004.